Article
Vol. 22, No. 1, p. 145–154, February 2018
http://dx.doi.org/10.1007/s12303-016-0072-3
pISSN 1226-4806 eISSN 1598-7477
Geosciences Journal GJ

Structural control of hydrogeological aquifers in the Bahariya Oasis, Western Desert, Egypt

Taha Rabeh[1], Said Bedair[2], and Mohamed Abdel Zaher[1]*

[1]National Research Institute of Astronomy and Geophysics, Helwan, Cairo 11421, Egypt
[2]National Water Research Center, PO Box 74, Shobra El-Kheima, Cairo 13411, Egypt

ABSTRACT: This work addresses the detection of aquifers and the delineation of subsurface structures predominant in the basement rocks and their relations with these aquifers at the Bahariya Oasis, Western Desert, Egypt, and the relationship between the subsurface structures and the aquifers. In this respect, land geomagnetic and geoelectric-reconnaissance surveys were carried out over the oasis. Additionally, wells and bore-hole logs were used to verify the results and to explore the distributions of the subsurface reservoirs and the geological sequences. The results illustrate that the main groundwater aquifers in the fractured limestone ranges from 40 m to 90 m in depth and in the saturated Nubian sandstone from 800 m to 1200 m in depth. The thickness of the Carbonate reservoir varies from 90 m to 160 m. The Nubian sandstone formation that unconformably overlies the basement rocks has a thickness of approximately 250 m. In general, the depth to the basement rocks ranges from 1.2 km and 2.9 km in certain local areas according to the magnetic data. The structure trend analyses show that the dominant tectonic trends are northeastward and northwestward. These structures play an important role in controlling the aquifer depths and most probably supply water from the deeper Nubian aquifer to the shallower Carbonate aquifer.

Key words: aquifer, reconnaissance surveys, geomagnetic, geoelectric, Nubian sandstone

Manuscript received March 7, 2016; Manuscript accepted September 18, 2016

1. INTRODUCTION

Egypt has a quickly growing population now surpassing 90 million, concentrated along the narrow Nile valley and delta. To support its increasing population, the government of Egypt has implemented major engineering projects in the western desert to manage its water resources and expand its agricultural territory. The western desert of Egypt occupies approximately 68% of the Egyptian surface area and is considered a strategic water resource in Egypt due to the groundwater of the Nubian aquifer being considered the sole source of water for sustainable development in the area. The western desert is characterized by the existence of several oases: e.g., Siwa, Bahariya, Farafra, Dakhla and Kharga (Fig. 1). The Bahariya Oasis is one of the most attractive sites for geologists and consists of many villages, the largest of which is El-Bawiti. It is delimited by latitudes 27°50′ and 28°30′N and longitudes 28°40′ and 29°10′E, covering an area of approximately 3575 km^2. The Bahariya Oasis is considered a part of the unstable shelf in Egypt and is characterized by extremely arid weather and deep marine sediments.

In this study, a land geomagnetic reconnaissance survey was carried out over the whole oasis, followed by a vertical electrical sounding (VES) for 18 stations along selected profiles to detect groundwater potentiality and structural elements controlling the geometry of the groundwater aquifers in the study area (Fig. 1). Additionally, a study was carried out using the information derived from four drilled wells distributed over the study area to verify the geophysical results from geomagnetic and geoelectric investigations.

Attraction studies have been broadly used as part of groundwater investigations where the detection of structures was the principal target (i.e., Al-Garni et al., 2005; Rabeh et al., 2011; Abdel Zaher et al., 2011; Saadi et al., 2011). For groundwater investigation, the electrical resistivity method, which uses the VES technique is extensively used due to the low resistivity of groundwater (i.e., Zohdy et al., 1989; Abdel Zaher et al., 2008;

*Corresponding author:
Mohamed Abdel Zaher
National Research Institute of Astronomy and Geophysics, Helwan, Cairo 11421, Egypt
Tel: +201159299090, E-mail: moh_zaher@yahoo.com

Massoud et al., 2010; Hewaidy et al., 2015).

Many groundwater investigation studies have been conducted in the western desert. El Kashouty et al. (2012) conducted VES and transverse electromagnetic (TEM) measurements in El-Bawiti in the northern Bahariya Oasis. The measurements gave detailed information about the geometry and depth of the different hydrogeological layers in the aquifer system. Abdel Zaher et al. (2014) delineated the major surface and subsurface structures to evaluate the tectonic framework of the southern part of the western desert of Egypt that control the geometry of subsurface aquifers. Abd El All et al. (2015) delineated the shallow and deep subsurface structures at the Bahariya Oasis using two geophysical methods: geomagnetic and geothermal investigations.

2. GEOLOGICAL AND TECTONIC SETTING

The Bahariya Oasis in the Western Desert in Egypt is situated 370 km southwest of Cairo. The exposed stratigraphic sequence in the Bahariya Oasis ranges from Cretaceous to Quaternary

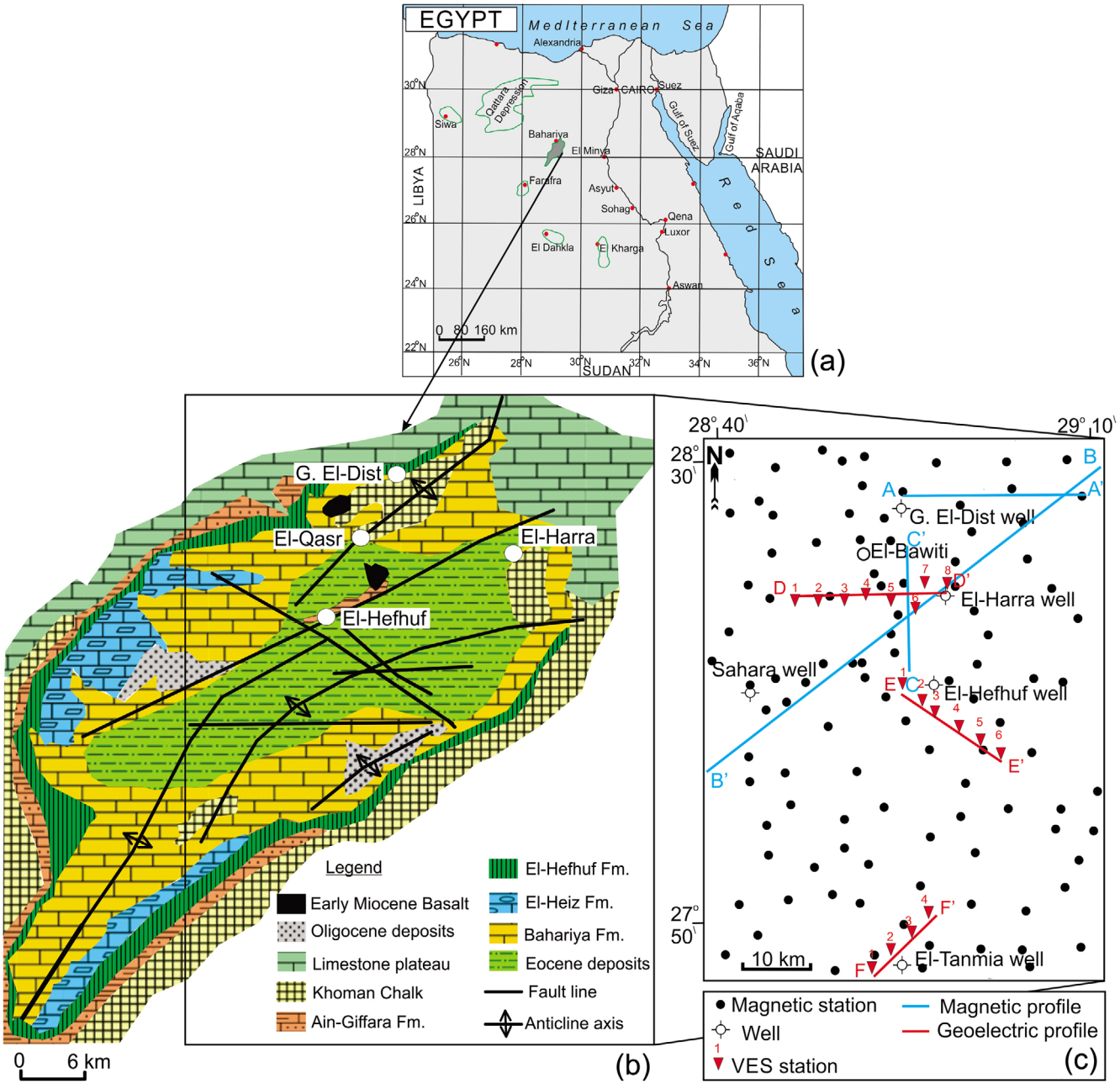

Fig. 1. (a) Location map of Egypt showing the distributions of oases in the Western Desert, (b) the geologic map of the Bahariya Oasis (El Akkad and Issawi, 1963), and (c) the locations of magnetic and VES measured stations.

(Fig. 1b). The Cretaceous rocks in this region are differentiated into the Bahariya, El-Heiz, El-Hefhuf, Ain-Giffara and Khoman/Chalk Formations (Said, 1962; El-Akkad and Issawi, 1963; Khalifa, 1977). Early Cenomanian sediments (Bahariya Fm.) are unconformably overlain by Middle Eocene rocks, which in turn are overlain by the Oligocene Radwan Formation (El-Akkad and Issawi, 1963; Said and Issawi, 1966). The entire sedimentary sequence is injected with Tertiary basalts and dolerites that occur in the form of sills and dykes. Quaternary sediments are represented by aeolian sands and lacustrine deposits, with some recent continental sabkhas.

The Bahariya Oasis is considered to be an eroded anticlinal folds formed during the so-called Syrian arc movements (Shukri, 1954). Synclinal folds within Bahariya Oasis are separated by anticlinal structures trending in the NE-SW direction. Three trends of folds as well as faults are recorded in the Bahariya Oasis: the NE-SW, E-W, and NW-SE directed, the latter of which disturbs the younger formations (Middle Eocene) in the northern part of the Bahariya depression (El-Akkad and Issawi, 1963). Faults crossing the study area mostly consist of two sets of NE and NW faults crossing the axes of the folds (Issawi, 1968).

3. MEASUREMENTS AND DATA ACQUISITION

This work was performed in three stages: land magnetic surveys, geoelectric surveys, and well logging interpretations. Surveys were carried out in August–September 2012. A detailed land magnetic survey using two proton magnetometers of Geometrics type G-856 in a mesh-like network was undertaken in the Bahariya Oasis. One proton magnetometer was fixed at a selected base station in a quiet magnetically anomalous area. The second proton magnetometer was used to measure the intensity of the magnetic field along the surveyed area. The survey process was performed for the observed stations along north-south and east-west traverses covering the study area. The spacings between the survey stations range 2000 meters to 3000 meters depending on magnetic field variations and terrain-induced obstacles. The locations of the measured stations were confirmed using a global positioning system (GPS) instrument with an accuracy of approximately 1 m. The necessary corrections for the observed magnetic data (e.g., IGRF, annual correction, pole reduction, and upward continuation) were made.

Two methods of geoelectric surveys were used in the investigation: a capacitively-coupled resistivity survey using a Geometrics Ohm-Mapper TR-5 instrument, and a VES survey using a Syscal Junior R72 (IRIS) instrument. Resistivity measurements from the Ohm-Mapper TR-5 were used to assess the physical parameters of the subsurface materials. The Ohm-Mapper TR-5 has a simple coaxial-cable array with transmitter and receiver section that are pulled, in this case by a surveyor, along east–west profiles covering the study area. The system is unique in that it does not require direct coupling with the ground but rather, in a capacitively-coupled resistivity meter, the transmitter uses the antenna's capacitance to couple an AC signal into the ground. Data collection is many times faster than for systems using conventional DC resistivity. A series of measurements were made along a traverse with a constant transmitter-receiver separation of approximately 10 m. The transmitter-receiver separation distance is primarily determined by the length of the cable – a longer cable has a greater capacitance. The VES survey was carried out with a Syscal Junior R72 (IRIS) instrument using a Schlumberger array. The measurements were performed in profile form at approximately 18 VES stations (Fig. 1c).VES measurements are based on measuring the potentials between one electrode pair while transmitting direct current (DC) between another electrode pair. This movement signifies an increased depth measurement as the current electrodes are moved farther apart. This depth is proportional to the separation between the electrodes in homogeneous ground, and varying the electrode separation provides information about the stratification of the ground (Dahlin, 2001). The well logging data were used to illustrate the sediment successions and to analyze their properties. The main purpose for drilling these wells is to determine the aquifer's water distribution, water level, and subsurface geology of the area, as well as the presence or absence of petroleum. The maximum depth was for the petroleum exploration well drilled by the American Sahara Petroleum Company (SAPETCO) in 1956. The geologic data and the resulting rock analysis of the drilled wells were used to construct the subsurface geology and structures of the area.

4. DATA ANALYSES AND RESULTS

4.1. Magnetic Data

The purpose of measuring the earth's magnetic field intensity is to delineate the subsurface fault trends and structures responsible for recharging the aquifers in the study area. Due to changes in the declination and inclination angles of the magnetic vector, there will be a shift in the location of the magnetic anomalies of the subsurface source on the map. Therefore, the reduction-to-the-pole (RTP) technique of Mendonca and Silva (1993) has been applied to the total magnetic intensity map to produce the RTP magnetic map (Fig. 2).

The theory of the first horizontal gradient methods has

http://dx.doi.org/10.1007/s12303-016-0072-3

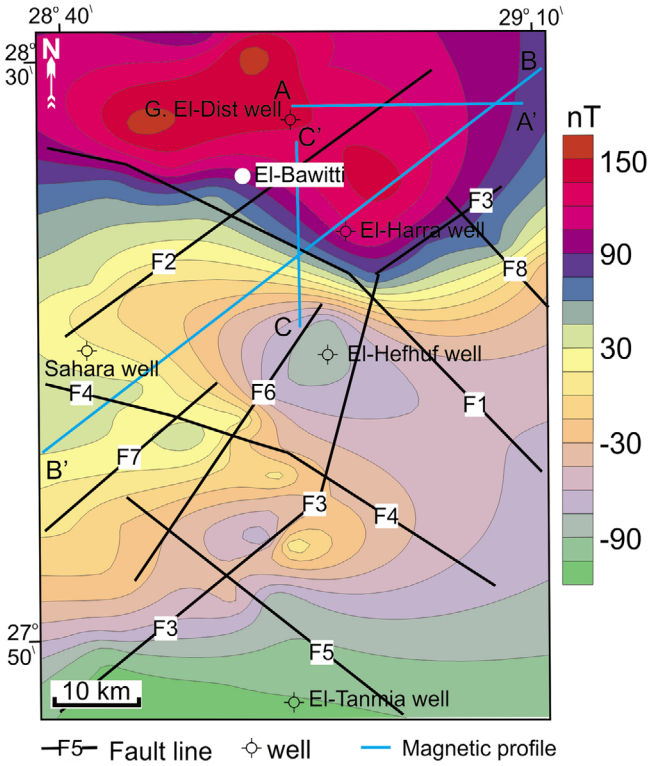

Fig. 2. RTP land magnetic map surveyed using two proton magnetometers of Geometrics type G-856. The black lines indicate faults deduced from trend analyses of the horizontal gradient along several profiles, blue lines refer to magnetic profiles while the red line refer to the geoelectric profiles.

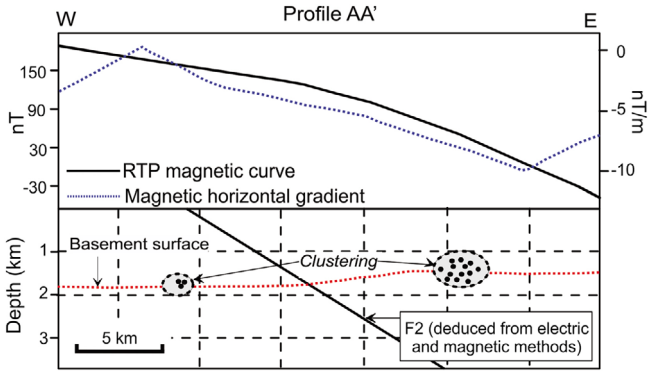

Fig. 3. Werner deconvolution showing the depth to the basement rock and the subsurface structures confirmed by analytical signals along Profile A–A' as shown in Figure 2.

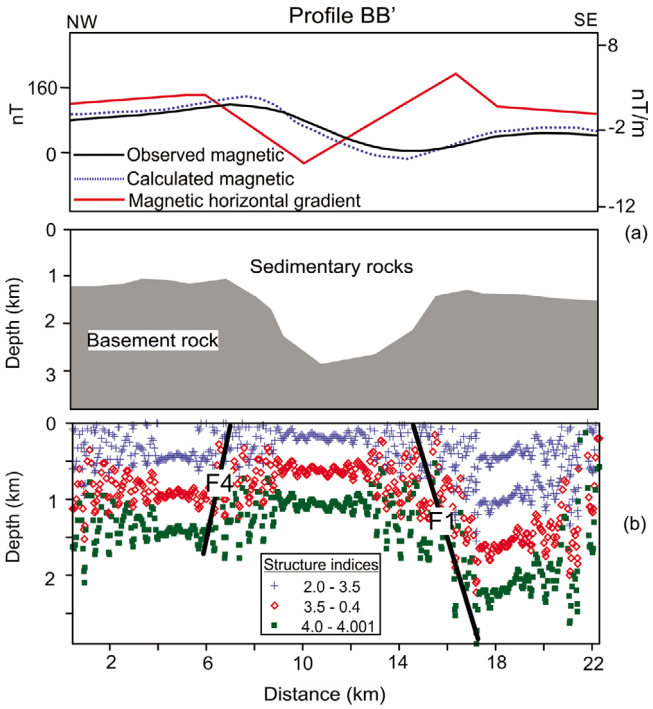

Fig. 4. (a) 2.5D magnetic model along B–B'. The horizontal x-axis represents the distance in meters along the profile; the vertical axis is the magnetic field in nT. The lower section represents the geological model results from fitting of the observed (dotted line) and calculated (solid line) data and the red line refers to horizontal gradient. (b) 2D Euler deconvolution along profile B–B' confirming the presence of the two faults F1 and F4 deduced by geoelectric and magnetic interpretations.

been applied to the RTP magnetic map to evaluate the subsurface structures and geometry of the basement surface in the study area. Several authors have developed various methods for detecting edges based on the use of horizontal or vertical gradients of potential-field anomalies (Grant and West, 1965; Linsser, 1967; Grauch and Cordell, 1987; Reid et al., 1990; Roest et al., 1992; Hsu et al., 1996; Fedi and Florio, 2001). We analyzed the horizontal gradient along several profiles covering the study area and plotted and connected the resulting peaks of the gradient curve to show the deduced structure lines. The different directions were then grouped into segments of 10° of azimuth each. The magnetic data were also used to determine the depth to the basement rocks and the thickness of the sedimentary cover along the study area using Euler and Werner deconvolution, 2.5D modeling and power spectrum methods. The Werner method (Werner, 1953) was also applied on profile A–A' based on successive determinations of small dykes with infinite strike length and depth extent, perpendicular to the measurement profiles, which could be considered the source of the magnetic anomaly described by a set of four or more contiguous measurements. In addition, horizontal gradient analysis was performed for the Werner magnetic profile A–A' to confirm the deduced structures (Fig. 3). The results of these methods show that the depth of the structures ranges from 1.8 km to approximately 2.5 km.

The 2.5D modeling based on Talwani (1965) shows that the depths to the basement rocks ranges from 1.2 km at the northwestern corner of the study area to approximately 2.9 km in the middle of the area (Fig. 4a). The Euler deconvolution method (Hsu, 2002; Stavrev, 1997; Cooper and Cowan, 2003) was

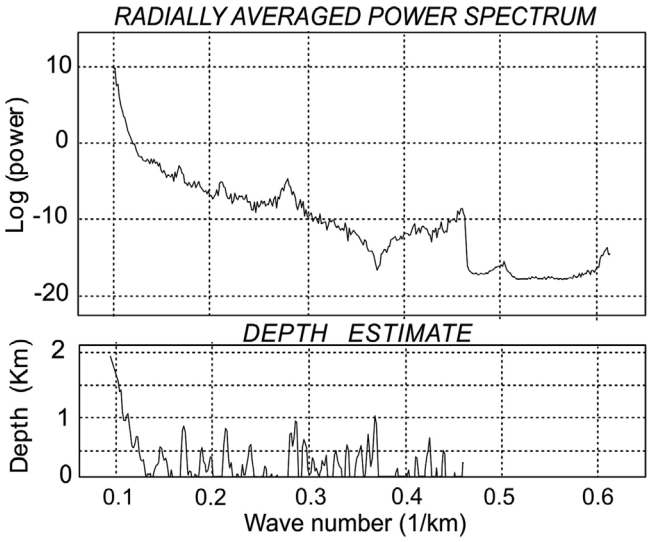

Fig. 5. Radially averaged power spectrum of the RTP land magnetic map of the study area illustrating the depth to the basement rocks.

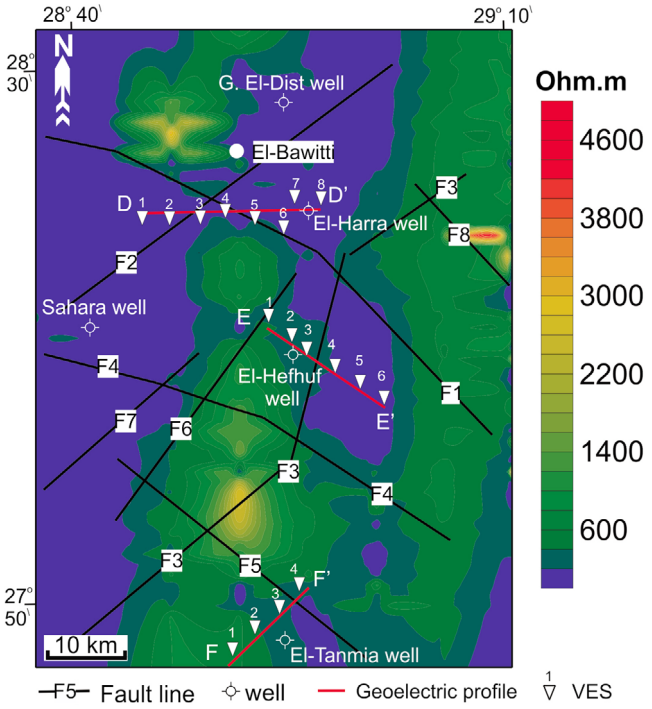

Fig. 6. Shallow resistivity map deduced from the geoelectric survey using the Geometrics Ohm-Mapper TR-5 instrument.

applied to the vertical gradient of the total magnetic field and serves to determine source positions and depths of the magnetic contrasts. The results along magnetic profile B–B' (Fig. 4b) were correlated with the structures deduced from the trend analysis. The depth to the basement rock was also calculated by estimating the radial averaged power spectral of the magnetic anomalies. The theoretical basis of estimating the depth from Fourier spectra has been explained by several authors such as Bhattacharyya (1966), Spector (1968), Spector and Grant (1970), and Hahn et al. (1976). The algorithm given by Spector and Grant (1970) shows the radially averaged power spectrum curve (Fig. 5) and the corresponding depth estimate, which reaches approximately 1.9 km and agrees with the data derived from the Sahara well drilled in 1956 by the SAPETCO to a depth of approximately 1.84 km.

4.2. Geoelectric Data

Multiple Ohm-Mapper TR-5 survey line setups, measuring resistivity at shallower depths, were integrated to provide a resistivity map for the study area (Fig. 6) that shows the resistivity depth of up to 10 m. The results show that the area is saturated by water rich with dissolved minerals. The areas of lowest resistivity are located near the western edge of the study area and in some isolated areas in the central and southeastern parts.

The field data from VESs were analyzed with a computer

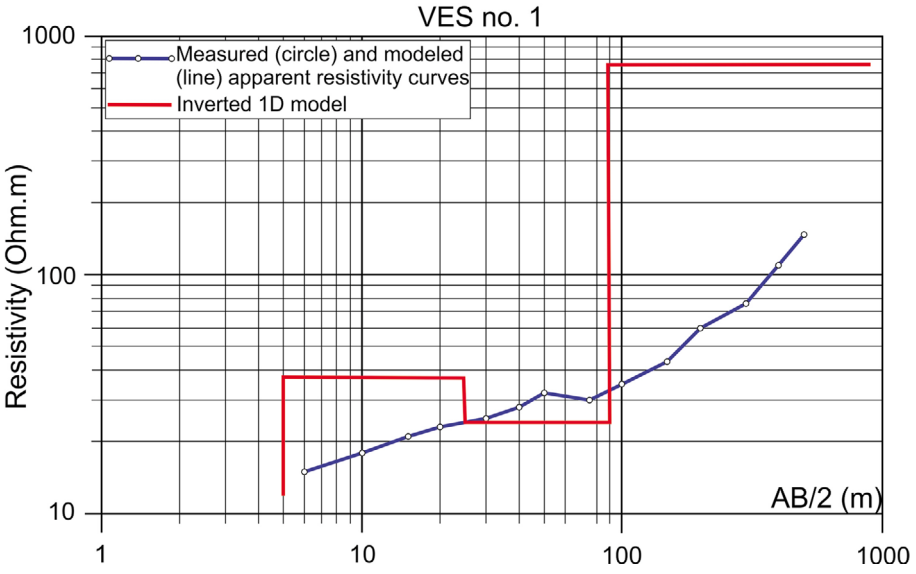

Fig. 7. Example of the result of the application of the Zohdy method (1989) to VES Station No. 1 to determine the geoelectric layers.

http://dx.doi.org/10.1007/s12303-016-0072-3

Table 1. Results of the application of the Zohdy method (1989) on VES Station No. 1 to determine the geoelectric layers

Layer No.	1	2	3	4	5
True resistivity (Ωm)	41	110	115	55.4	450
Thickness (meter)	5	5.32	44.13	150	–
Depth to the bottom of the layers (meters)	5	18.5	55	180	–

program by Zohdy (1989). This computer program uses field-measured data of apparent resistivity and electrode spacing to generate a vertical assemblage of iso-resistivity units known as an inverse model. This model can be displayed and interpreted as a form of geoelectric layers. An example of the application of this method for VES Station No. 1 is illustrated by Figure 7 and Table 1. Six lithological layers above the fresh basement rocks have been recognized and can be described in terms of geoelectric cross-sections based on lithological information from well data.

Geoelectric profile D–D' (Fig. 8), located south of El-Bawiti and running from east to west, shows that the main aquifer is

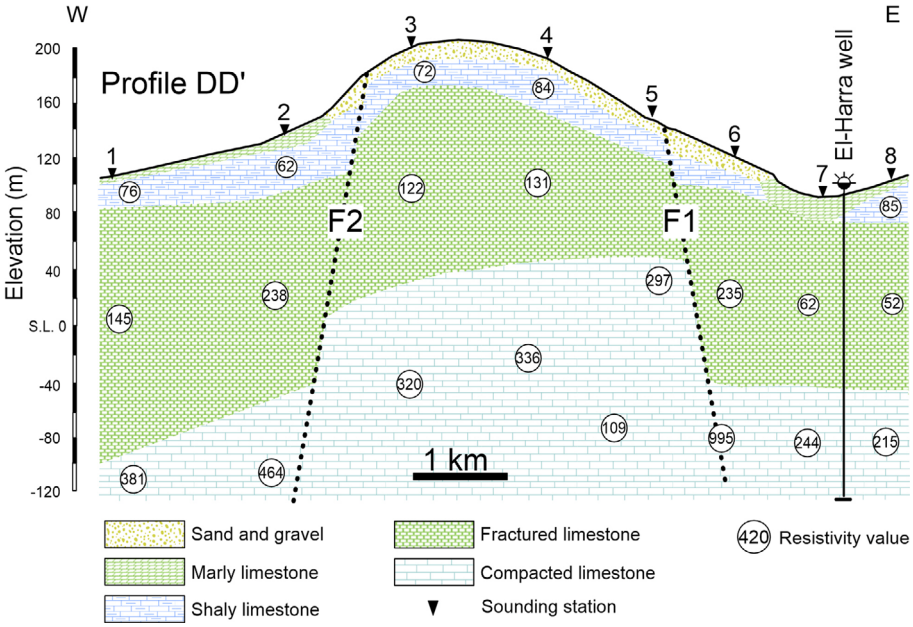

Fig. 8. Geoelectric cross section along profile D–D' shows that the main aquifer is represented by the lower layer (fractured limestone), and the El-Harra well was used to verify the result.

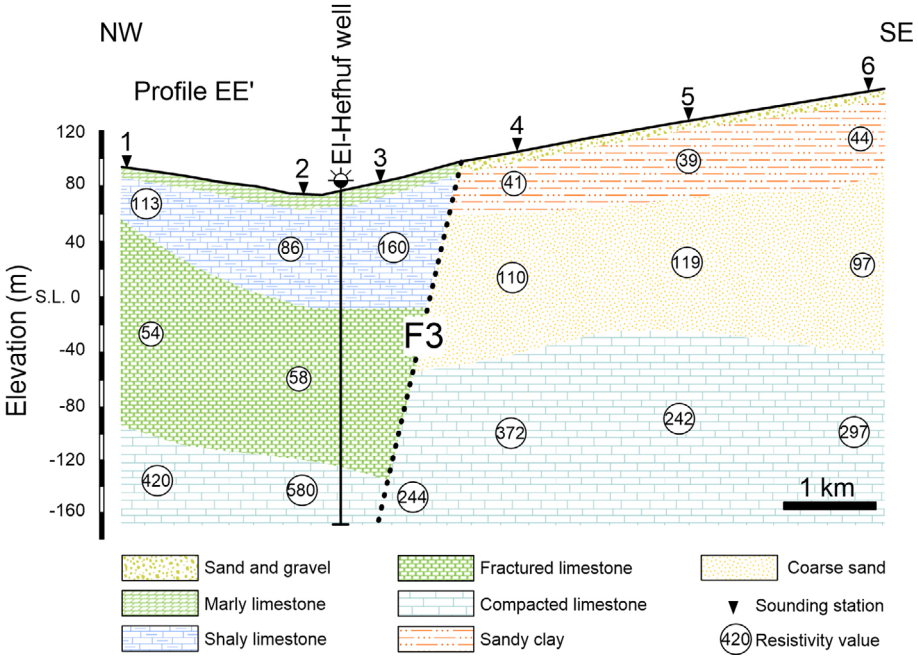

Fig. 9. Geoelectric cross section along profile E–E' shows that the main aquifer is represented by the lower layer (fractured limestone). The result was verified using data from the El-Hefhuf well.

represented by the middle geoelectric layer (fractured limestone). The resistivity ranges from 238 Ohm-m in the southern part of the study area to approximately 52 Ohm-m in the eastern part (the El-Harra well). The wide range of resistivity is due to variation in the facture intensity causing variation in porosity, permeability and pore connectivity geometries. The upper layer shows the lowest resistivity (60 Ohm-m) that is correlated with the low resistivity deduced from Geometrics' Ohm-Mapper map (Fig. 6). The base layer characterized by high resistivity value referring to compacted limestone surface and appears to be affected by two fault lines (F2 and F1).

Geoelectric profile E–E' (Fig. 9) runs from northwest to southeast for a distance of 8 km. A close inspection of this profile reflects that it is affected by the F3 fault line. The compacted limestone layer is noticeably shallower at the southeastern part of the profile. These results are confirmed by the data from the El-Hefhuf well. The low resistivity of the upper geoelectric layer at the southeastern part of the profile is also correlated with the low resistivity deduced from the Geometrics Ohm-Mapper map (Fig. 7). Additionally, they confirm the data deduced from the drilled wells.

Geoelectric profile F–F' (Fig. 10) is 5 km long and runs from southwest to northeast. A close inspection along this profile reflects that it is affected by the F5 fault line. The compacted limestone layer is noticeably shallower at the southeastern part of the profile. These results are confirmed by the data from the El-Tanmia well. The low resistivity of the upper geoelectric layer along the profile is also correlated with the Geometrics Ohm-Mapper map (Fig. 6).

5. INTERPRETATION AND DISCUSSION

The obtained results from geoelectric and magnetic data illustrate that the depths to the main water aquifers represented by the fractured limestone range from 40 m to 90 m and that the depths to the saturated Nubian sandstone ranges from 800 m to 1200 m. The thickness of the Carbonate reservoir varies from 90 m to 160 m. The Nubian sandstone formation unconformably overlies the basement rocks and has a thickness of approximately 250 m. In general, the depth to the basement rocks reaches approximately 1200 m and 2900 m in some local areas as interpreted from magnetic data. The structure trend analyses show that the dominant tectonic trends are northeastward and northwestward. The structural development of the central Sahara follows fairly regular patterns, with an older northwestward-striking pattern and a younger one with an approximately northeastward orientation (Klitzsch, 1986). These structures play an important role in controlling the depths of the aquifers and most probably supply water from the deeper Nubian aquifer to the shallow Carbonate aquifer. Furthermore, a correlation exists between the locations of the faults deduced along the geoelectric cross sections and the locations deduced from the magnetic trend analysis, interpreting that these faults are due to basement tectonics. The results from magnetic data illustrate that the study area is affected by two groups of faults having northwestward and northeastward directions (Fig. 2). These faults extend from the surface to the basement rocks. From the correlation of the locations of deduced faults and water resources, it appears that these faults are primarily responsible for the conduction and recharging of the water aquifers from

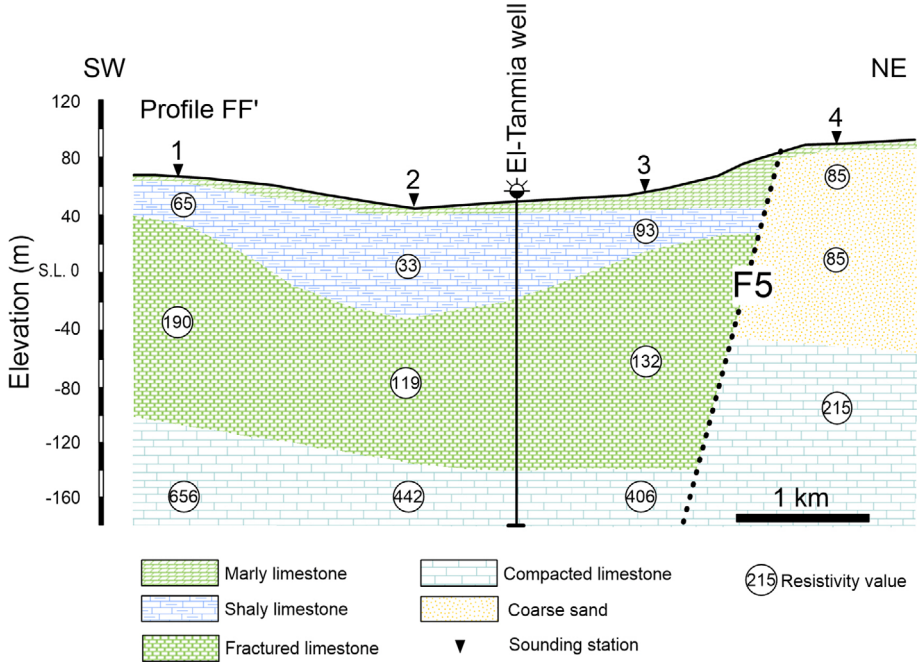

Fig. 10. Geoelectric cross section along profile F–F' shows that the compacted limestone layer is relatively shallower at the southeastern part of the profile. The El-Tanmia well was used for verifying the result.

http://dx.doi.org/10.1007/s12303-016-0072-3

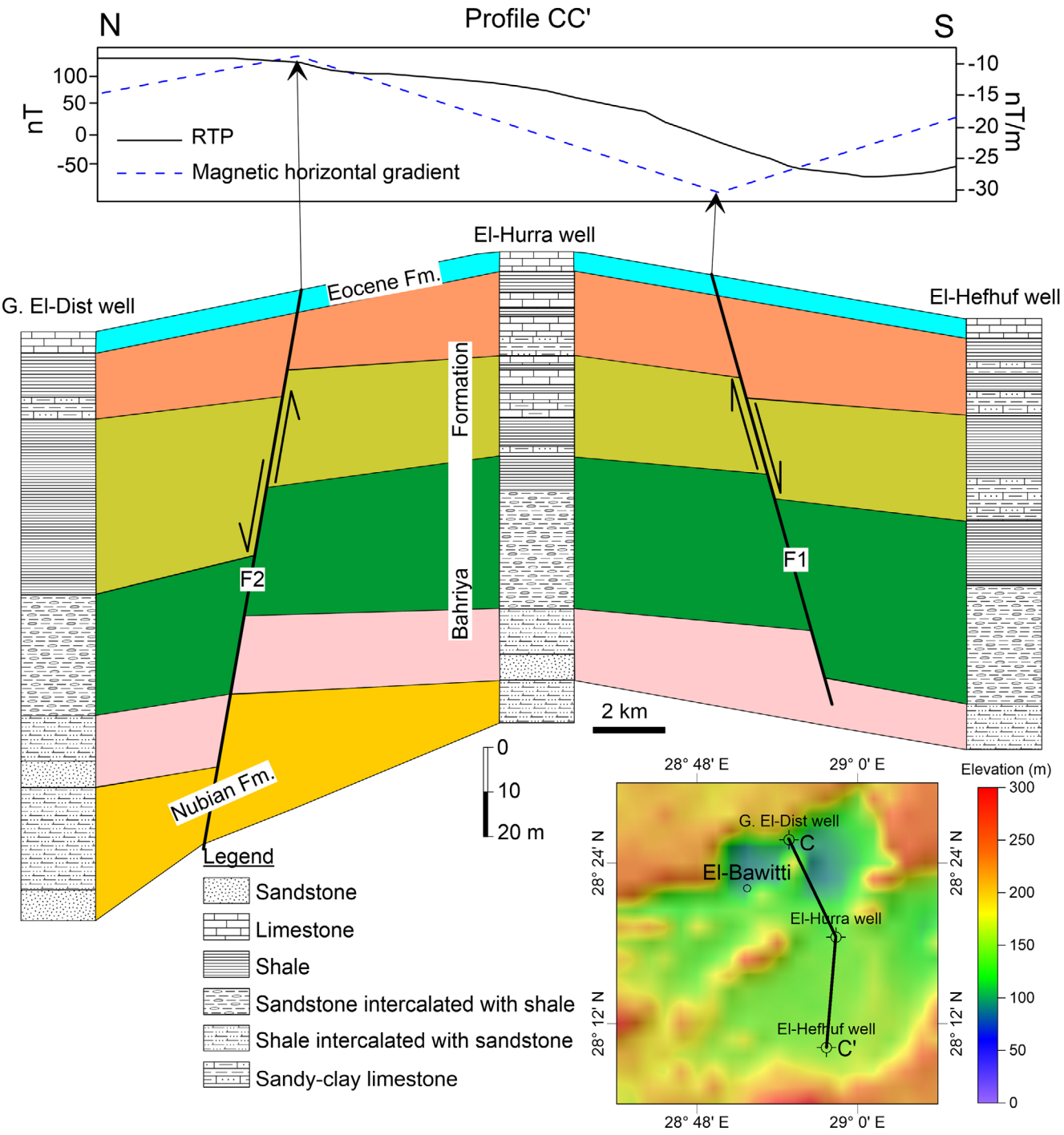

Fig. 11. Composite geologic cross section from lithological well logs supported by the RTP magnetic profile and the horizontal gradient curve along profile C–C'. The lower map shows the location of the profile C–C' on a topographic map of study area (DEM from a satellite dataset).

the deeper Nubian aquifer.

The Bahariya Formation, the type locality of which is situated in Gebel El-Dist, forms the floor of the Bahariya Oasis and constitutes all the isolated hills within the oasis. The well logging interpretations along magnetic profile C–C' show that the Bahariya Formation overlies the Nubian sandstone formation. Four depositional sequences have been recognized for the Bahariya Formation in the Bahariya depression, separated by three sub-aerial unconformities. These unconformities might be related to tectonic uplift associated with the development of the Syrian Arc System between the Upper Cenomanian (El-Heiz Formation) and Maastrichtian (Khoman Chalk) interval (El Emam et al., 1990). The lowest depositional sequence is shale intercalated with sandstone at the bottom; the second is compacted

Table 2. Summary of results from geomagnetic, geoelectric, and lithological well data for identifying different layers in the study area

Layers	Average thickness (m)	Method used for identification	Resistivity (Ohm.m)
Surface deposits (gravel, sand and gravelly sand)	10	Geoelectric + wells	93–135
Shaly limestone	50	Geoelectric + wells	33–160
Fractured limestone	100	Geoelectric + wells	54–238
Clayey sand	30	Geoelectric + wells	39–44
Coarse sand	70	Geoelectric + wells	97–119
Compacted limestone	–	Geoelectric + wells	97–119
Nubian sandstone	800–1200	Magnetic + wells	–
Basement rock	1200–2900	Magnetic + wells	–

limestone; the third fractured limestone representing the main shallow water aquifer; and the highest shelly limestone (Fig. 11). The results from geoelectric profiles show that the upper layer has lowest resistivity due to seepage of irrigated water and dissolved salt minerals, whereas the lower layer has higher resistivity values and is correlated with compacted limestone. This compacted limestone affected by fault lines in all profiles (F1, F2 in profile D–D', F3 in profile E–E', and F5 in profile F–F'), which interpreted by the sudden appearance of a layer of high resistivity whose depth was confirmed by drilled wells. The southeastern part of profile E–E' characterized by low resistivity values due to the existence of a water-rich sandy clay layer.

The four sequences overlie the main Nubian aquifer and rest below El-Heiz Formation (Tanner and Khalifa, 2010). The Nubian sandstone members can be described as follows from bottom to top in agreement with Tanner and Khalifa (2010): (1) shale intercalated with sandstone at the base of the Bahariya sequence overlying the Nubian sandstone; (2) compacted limestone containing stratified limestone; (3) fractured limestone representing the main body of the shallow aquifer and possessing high porosity and permeability; and (4) shelly limestone consisting of an intercalation of shale and limestone at the top of the Bahariya sequence.

6. CONCLUSIONS

The study area lies in the western desert of Egypt approximately 360 km southwest of the capital, Cairo. It is considered a part of the unstable shelf of Egypt. Geophysical measurements were carried out to detect the aquifers and the subsurface structures controlling the water and recharging the aquifers in the study area. In this respect, three tools have been used: (1) drilled wells enabled us to determine the geologic sequences and the depth to the water aquifer (fractured limestone); (2) the land magnetic survey enabled us to determine the depth to the basement rocks and the subsurface structures affecting the studied area; and (3) finally, a geoelectric shallow-depth resistivity and VES survey allowed us to determine the exact carbonate aquifer carrier member (saturated surface layers and fractured limestone aquifer) and its extension along the studied area. The third tool confirmed the results obtained from the well logging and geomagnetic surveys. Table 2 shows the conclusion of our results representing identification of different layers using geophysical and well data. The obtained results also illustrated that basement rocks have been affected by two predominant sets of fault systems trending in the northeastward and northwestward directions. Furthermore, the correlation of the locations of these faults and water resources shows that these faults are probably responsible for conducting and recharging the carbonate aquifers from the deeper Nubian aquifer. This work presented in this study should help further exploration.

ACKNOWLEDGMENTS

The authors are grateful to Dr. Gwang Hoon Lee, editor of Geosciences Journal and the anonymous reviewers who spent hours/days of their personal time on our manuscript to make it suitable for publication in Journal. Also, we would like to highly appreciate Research Institute for Groundwater (RIGW), National Water Research Center (NWRC) for their supporting to achieve this work.

REFERENCES

Abd El All, E., Khalil, A., Rabeh, T., and Osman, S., 2015, Geophysical contribution to evaluate the subsurface structural setting using magnetic and geothermal data in El-Bahariya Oasis, Western Desert, Egypt. NRIAG Journal of Astronomy and Geophysics, 4, 236–248.

Abdel Zaher, M., Saadi, N.M., and Wananabe, K., 2014, Geological applications potential of DEM, ETM+, and gravity data in arid and semi-arid regions with special reference to south Western Desert, Egypt. Arabian Journal of Geosciences, 7, 1705–1716.

Abdel Zaher, M., Saibi, H., El Nouby, M., Ghamry, E., and Ehara, S., 2011, A preliminary regional geothermal assessment of the Gulf of Suez, Egypt. Journal of African Earth Science, 60,117–132.

Abdel Zaher, M., Sultan, A.S., El-Said A.A., and Ehara, S., 2008, Geophysical Study of the Sedimentary Cover in Darb El-Arbeen, South Western Desert, Egypt. Memoirs of the Faculty of Engineering, Kyushu University, 68, 83–92.

Al-Garni, M.A., Hassanein, H.I., and Gobashy, M.M., 2005, Ground-

 http://dx.doi.org/10.1007/s12303-016-0072-3

magnetic survey and Schlumberger sounding for identifying the subsurface factors controlling the groundwater flow along Wadi Lusab, Makkah Al-Mukarramah, Saudi Arabia. Journal of Applied Geophysics, National research institute, Egypt, 4, 59–74.

American Shara Petroleum Co. (SAPETCO), 1956, Project of oil exploration at the northwestern Desert of Egypt, well logging drilled data. Internal report.

Bhattacharyya, B.K., 1966, Two-dimensional harmonic analysis as a tool for magnetic interpretation. Geophysics, 30, 829–875.

Cooper, G.R.J. and Cowan, D.R., 2003, The application of fractional calculus to potential field data. Exploration Geophysics, 34, 51–56.

Dahlin, T., 2001, The development of DC resistivity imaging techniques. Computers Geosciences, 27, 1019–1029.

El-Akkad, S. and Issawi, B., 1963, Geology and iron ore deposits of Bahariya Oasis. Geological Survey of Egypt, Cairo, Paper No. 18, 300 p.

El Emam, A., Dishopp, D., and Dunderdale, I., 1990, The structural setting of the central Western Desert, Egypt. Proceedings of the 10th Egyptian General Petroleum Corporation Seminar, Cairo, Nov. 19–22, 2, p. 30–70.

El Kashouty, M., Abdel Aziz, A., Soliman, M., and Mesbah, M., 2012, Hydrogeophysical investigation of groundwater potential in the El-Bawiti, Northern Bahariya Oasis, Western Desert, Egypt. Arabian Journal of Geosciences, 5, 953–970.

Fedi, M. and Florio, G., 2001, Detection of potential fields source boundaries by enhanced horizontal derivative method. Geophysical Prospecting, 49, 40–58.

Grant, F.S. and West, G.F., 1965, Interpretation theory in applied geophysics. McGraw Hill, New York, 584 p.

Grauch, V.J.S. and Cordell, L., 1987, Limitations of determining density or magnetic boundaries from the horizontal gradient of gravity or pseudogravity data. Geophysics, 52, 118–121.

Hahn, A., Kind, E.G., and Mishra, D.G., 1976, Depth estimation of magnetic sources by means of Fourier amplitude spectra. Geophysical Prospecting, 24, 287–308.

Hewaidy, A.A., El-Motaal, E.A., Sultan, A.S., Ramdan, T.M., El khafif, A.A., and Soliman, S.A., 2015, Groundwater exploration using resistivity and magnetic data at the northwestern part of the Gulf of Suez, Egypt. Egyptian Journal of Petroleum, 24, 255–263.

Hsu, S.K., 2002, Imaging magnetic sources using Euler's equation. Geophysical Prospecting, 50, 15–25.

Hsu, S.K, Sibuet, J.C., and Shyu, C.T., 1996, High-resolution detection of geologic boundaries from potential field anomalies: an enhanced analytic signal technique. Geophysics, 61, 373–386.

Issawi, B., 1968, The geology of Kurkur-Dungul area. Geological survey of Egypt, Paper No. 46, Cairo, 102 p.

Khalifa, M.A., 1977, Geological and Sedimentological Studies of the El-Hefhuf Area, Bahariya Oases, Western Desert, Egypt. M.Sc. Thesis, Cairo University, Cairo, 181 p.

Klitzsch, E., 1986, Plate tectonics and cratonal geology of Northeast Africa (Egypt, Sudan). Geologische Rundschau, 75, 755–768.

Linsser, H., 1967, Investigation of tectonic by gravity detailing. Geophysical Prospecting, 15, 480–515.

Mendonca, C.A. and Silva, J.B.C., 1993, A stable truncated series approximation of the reduction-to-the-pole operator. Geophysics, 58, 1084–1090.

Massoud, U., Santos, F., Khalil, M.A., Taha, A., and Abbas, A.M., 2010, Estimation of aquifer hydraulic parameters from surface geophysical measurements: a case study of the Upper Cretaceous aquifer, central Sinai, Egypt. Hydrogeology Journal, 18, 699–710.

Rabeh, T., Miranda, J.M.M., Carvalho, J., and Bocin, A., 2011, Interpretation case study of the Sahl El Qaa area, southern Sinai Peninsula, Egypt. Geophysical Prospecting, 57, 447–459.

Reid, A.B., Allsop, J.M., Granser, H., Millet, A.J., and Somerton, I.W., 1990, Magnetic interpretation in three dimensions using Euler deconvolution. Geophysics, 55, 80–91.

Roest, W.R., Verhoef, J., and Pilkington, M., 1992, Magnetic interpretation using the 3-D analytic signal. Geophysics, 57, 116–125.

Saadi, N.M., Abdel Zaher, M., El-Baz, F., and Watanabe, K., 2011, Integrated remote sensing data utilization for investigating structural and tectonic history of the Ghadames Basin, Libya. International Journal of Applied Earth Observation and Geoinformation, 13, 778–791.

Said, R., 1962, The Geology of Egypt. Elsevier, Amsterdam, 377 p.

Said, R. and Issawi, B., 1966, Preliminary results of a geological expedition to Lower Nubia and Kurkur and Dungul. In: Wendorf, F. (ed.), Contributions to the Prehistory of Nubia. Southern Methodist University Press, Dallas, p. 1–28.

Shukri, N.M., 1954, Remarks on the geological structure of Egypt. Geographical Society of Egypt Bulletin, 27, 65–82.

Spector, A., 1968, Spectral analysis of aeromagnetic data. Ph.D. Thesis, University of Toronto, Toronto, 239 p.

Spector, A. and Grant, F.S., 1970, Statistical models for interpreting aeromagnetic data. Geophysics, 35, 293–302.

Stavrev, P.Y., 1997, Euler deconvolution using differential similarity transformations of gravity or magnetic anomalies. Geophysical Prospecting, 45, 207–246.

Talwani, M., 1965, Computation with the help of a digital computer of magnetic anomalies caused by bodies of arbitrary shape. Geophysics, 30, 797–817.

Tanner, L.H. and Khalifa, M.A., 2010, Origin of ferricretes in fluvial-marine deposits of the Lower Cenomanian Bahariya Formation, Bahariya Oasis, Western Desert, Egypt. Journal of African Earth Sciences, 56, 179–189.

Werner, S., 1953, Interpretation of magnetic anomalies at sheet-like bodies. Sveriges Geologiska Undersökning, Serie C, Årsbok, 43, 130 p.

Zohdy, A.A.R., 1989, A new method for the automatic interpretation of Schlumberger and Wenner sounding curves. Geophysics, 54, 245–253.